University of Nebraska - Lincoln Digital Commons@University of Nebraska - Lincoln

Faculty Publications: Materials Research Science and Engineering Center

Materials Research Science and Engineering Center

1-1-2007

Dielectric anisotropy and phonon modes of ordered indirect-gap Al_{0.52}In_{0.48}P studied by farinfrared ellipsometry

Tino Hofmann University of Nebraska - Lincoln, thofmann4@unl.edu

V. Gottschalch University of Leipzig, Linnéstraße 3, 04103 Leipzig, Germany

Mathias Schubert University of Nebraska - Lincoln, mschubert4@unl.edu

Follow this and additional works at: http://digitalcommons.unl.edu/mrsecfacpubs



Part of the Materials Science and Engineering Commons

Hofmann, Tino; Gottschalch, V.; and Schubert, Mathias, "Dielectric anisotropy and phonon modes of ordered indirect-gap Al_{0.52}In_{0.48}P studied by far-infrared ellipsometry" (2007). Faculty Publications: Materials Research Science and Engineering Center. Paper

http://digitalcommons.unl.edu/mrsecfacpubs/61

This Article is brought to you for free and open access by the Materials Research Science and Engineering Center at DigitalCommons@University of Nebraska - Lincoln. It has been accepted for inclusion in Faculty Publications: Materials Research Science and Engineering Center by an authorized administrator of DigitalCommons@University of Nebraska - Lincoln.

Dielectric anisotropy and phonon modes of ordered indirect-gap $Al_{0.52}ln_{0.48}P$ studied by far-infrared ellipsometry

T. Hofmanna)

Department of Electrical Engineering and Nebraska Center for Materials and Nanoscience, University of Nebraska-Lincoln, Nebraska 68588-0511 USA

V. Gottschalch

Institute of Inorganic Chemistry, Faculty of Chemistry and Mineralogy, University of Leipzig, Linnéstraße 3, 04103 Leipzig, Germany

M. Schubert^{c)}

Department of Electrical Engineering and Nebraska Center for Materials and Nanoscience, University of Nebraska-Lincoln, Nebraska 68588-0511 USA

(Received 12 August 2007; accepted 27 August 2007; published online 19 September 2007)

The infrared $(100-600 \text{ cm}^{-1})$ optical properties of partially CuPt-type ordered $\text{Al}_{0.52}\text{In}_{0.48}\text{P}$ deposited lattice matched on GaAs are studied by ellipsometry. The authors determine the ordinary and extraordinary dielectric functions and report on the evolution of the optical phonon mode frequencies of $\text{Al}_{0.52}\text{In}_{0.48}\text{P}$ as a function of the degree of ordering. In addition to the InP- and AlP-like phonon modes, they observe two alloy-induced phonon modes which are anisotropic upon CuPt ordering. The observed modes are associated to vibrations with E and A_1 symmetries. The alloy-induced phonon modes are useful for classifying the degree of ordering in this indirect band gap alloy. © 2007 American Institute of Physics. [DOI: 10.1063/1.2785949]

CuPt-type ordering has been observed and extensively studied in ternary and quaternary III-V compound alloy systems. It can, besides chemical effects due to alloying or effects due to lattice-mismatch-induced strain, drastically affect the physical properties of a solid solution and is therefore of crucial importance for correct tailoring of device constituent properties.

Among the quaternary III-V alloys grown lattice matched on GaAs, the $(Al_xGa_{1-x})_{0.52}In_{0.48}P$ is of particular interest. $(Al_xGa_{1-x})_{0.52}In_{0.48}P$ is the working horse material for optoelectronic devices such as light emitting and laser diodes, solar cells, etc., and precise information on orderinduced changes in the physical properties is eminent to ensure functionality and device performance. Most studies have concentrated on the end component Ga_{0.52}In_{0.48}P, but the knowledge concerning the influence of ordering on the physical properties of Al_{0.52}In_{0.48}P, abbreviated here as AlInP₂, is not exhaustive. Recently, it was observed in Raman backscattering experiments that the AIP-like LO mode scattering intensities for incident light polarization parallel and perpendicular to the [110] lattice direction scales linearly with the degree of ordering in the alloy. However, no experimental observation and quantification of the optical active phonon modes in spontaneously ordered AlInP2 has been published so far.

In spontaneous CuPt-type ordered AlInP₂ alloys, the Al atoms are located in common ($\overline{1}11$) or ($1\overline{1}1$) planes. The degree of ordering η , which depends on the growth conditions and substrate orientation, is commonly treated as the composition difference of subsequent cationic (or anionic) sublattice planes of the ordered supercell structure, i.e., η is

considered as the difference of In concentration in subsequent $(\bar{1}11)$ or $(1\bar{1}1)$ cation planes.²

Far-infrared (fir) spectroscopic ellipsometry (SE) has proven to be a very sensitive tool to investigate infrared active phonon modes and free carrier parameters (e.g., see Refs. 3–6), and this technique is applied here to determine the phonon modes of spontaneously CuPt-type ordered AlInP2 grown by metalorganic vapor phase epitaxy (MOVPE). We determine the dielectric anisotropy and extract the ordinary ϵ_{\perp} and extraordinary ϵ_{\parallel} FIR dielectric functions for polarizations perpendicular and parallel to the ordering direction of the spontaneously CuPt-ordered alloy.

We investigate a set of five samples with different degrees of CuPt-type ordering. The samples were composed of an AlInP₂ layer on top of a GaAs buffer layer deposited by MOVPE on n-type (001) GaAs substrate. The sample parameters are summarized in Table I. The ordering-induced valence band splitting $\Delta E_{\rm VBS}$ was determined by dark field spectroscopy. We used the quasicubic perturbation model described in detail in Ref. 8 in order to determine the degree of ordering η of the AlInP₂ layer using the $\Delta E_{\rm VBS}$ values listed in Table I.

Spectroscopic ellipsometry determines the complex reflectance ratio $\rho \equiv r_p/r_s = \tan \Psi e^{i\Delta}$, where r_p and r_s are the complex Fresnel reflection coefficients for light polarized parallel (p) and perpendicular (s) to the plane of incidence, respectively, and Ψ and Δ denote the commonly used real-valued ellipsometric parameters.

The FIR-SE experiments for wavenumbers from $100 \text{ to } 600 \text{ cm}^{-1}$, and with a resolution of 1 cm^{-1} were carried out using a prototype, rotating-analyzer, Fourier-transform-based ellipsometer, which was equipped with a He-cooled bolometer detector system. The measurements were carried out at two different sample orientations: the $[\overline{1}10]$ axis parallel to the plane of incidence (setup \mathcal{A}) and

a)Electronic mail: thofmann@engr.unl.edu

c)Electronic mail: schubert@engr.unl.edu

TABLE I. Sample parameters of the studied $Al_{0.52}In_{0.48}P$ layers. Best-model results for $Al_{0.52}In_{0.48}P$ layer thickness d and GaAs buffer layer thickness d are obtained from the fir-SE data analysis. The error limits, which correspond to 90% reliability, are given in parentheses.

Sample	A	B	C	D	E
T_g (°C)	720	760	720	720	720
f _{V/III}	253	384	253	253	281.6
Orientation	6°	6°	6°	2°	2°
	(111)Ga	(011)Ga	(011)Ga	(011)Ga	(011)Ga
$\Delta a/a \ (10^{-4})$	-4	+3	-4	-5	~ 0
ΔE_{VBS} (meV)	• • •	42	50	63	73
η	0	0.39	0.43	0.47	0.52
d (nm)	913(9)	880(6)	900(8)	330(5)	396(15)
d_{buffer} (nm)	167(20)	131(8)	173(9)	223(6)	130(22)

the $[\bar{1}10]$ axis perpendicular to the plane of incidence (setup \mathcal{B}) subsequently at angles of incidence Φ_a =50° and 70°. For these sample orientations, the off-diagonal Jones reflection matrix elements are zero (setup \mathcal{A}) or very small (setup \mathcal{B}) and, therefore, the generalized ellipsometry procedure, needed otherwise for arbitrary optical axis orientations, can be avoided. ¹⁰

 Ψ and Δ , measured on layered samples, depend, in general, on all materials' dielectric functions including their directional dependencies (anisotropy), layer thickness values, and the incident wavelengths. In order to derive these quantities from SE data, model calculations are needed. The physical material parameters follow from an appropriately chosen parametrized model dielectric function (MDF) $\epsilon(\omega)$ for each layer. A three-phase model (Te doped, *n*-type GaAs substrate/undoped GaAs buffer layer/AlInP₂ layer) is employed here. The GaAs substrate and buffer layer are treated isotropic, and the AlInP₂ epilayer is modeled as a uniaxial layer. The fir-MDF used here consists of contributions due to polar lattice vibrations $\epsilon^{L}(\omega)$ and free charge carriers $\epsilon^{FC}(\omega)$, if present. A Lorentzian-broadened oscillator approach is used to model $\epsilon^L(\omega)$. $\epsilon^{FC}(\omega)$ is described using the classical Drude approximation for a single-specie free-carrier plasma.

The following parameters, denoted according to Ref. 12 are used to calculate $\epsilon(\omega)$ for the *n*-type doped GaAs substrate, and for the undoped GaAs buffer $\omega_{\rm TO}$ =267.9 cm⁻¹, $\omega_{\rm LO}$ =291.4 cm⁻¹, $\gamma_{\rm TO}$ = $\gamma_{\rm LO}$ =2.8 cm⁻¹, and ϵ_{∞} =11.0. The thickness of the buffer $d_{\rm buffer}$ and the AlInP₂ layer d are also adjustable parameters of significance given in Table I. The optical constants of the AlInP₂ layer obtained by the same best-fit regression analysis are discussed below.

The spontaneously ordered AlInP₂ layer is anisotropic and the ordering occurs as a single subvariant in the $[\bar{1}11]$ direction only. The optical response is that of a uniaxial material, with the optical axis collinear to the $[\bar{1}11]$. Hence, the dielectric tensor $\epsilon(\omega,\eta)$ may be diagonalized and ordinary and extraordinary dielectric functions for polarization perpendicular and parallel to the ordering direction can be assigned, denoted here by ϵ_{\perp} and ϵ_{\parallel} , respectively.

For perfect ordering, lattice modes split into those with A_1 - and E-type symmetries, with lattice displacement pattern parallel and perpendicular to the trigonal axis, respectively. For $0 < \eta < 1$ the trigonal lattice is not perfect. However, we keep the mode assignment for those found with polarization parallel (A_1) and perpendicular (E) to $[\overline{1}11]$. This assignment is distinct and unambiguous because we will derive these

modes from the dielectric functions ϵ_{\perp} and ϵ_{\parallel} , observed through the fir-SE experiment and subsequent data analysis.

In order to accurately model the components of the dielectric tensor $\epsilon(\omega,\eta)$, we employed two anharmonic oscillator functions with Lorentzian-type broadening to account for the contribution of AlP- and InP-like lattice vibrations. Furthermore, the contributions of the CuPt_B ordering-induced modes are treated in a convenient manner within the anharmonic oscillator approximation, as suggested by Kasic *et al.*⁵ The designation of phonon mode frequencies and broadening parameters is according to Eq. (1) in Ref. 5.

The experimental (dashed line) and calculated (solid line) fir-SE Ψ spectra for the sample orientations $\mathcal A$ and $\mathcal B$ at Φ_a =70° for the sample with the highest degree of ordering (E) are shown in Fig. 1. The spectrum measured with the sample [$\bar{1}$ 10] axis perpendicular and parallel to the plane of incidence are denoted with $\Psi_{\mathcal A}$ and $\Psi_{\mathcal B}$, respectively.

The reststrahlen band of the *n*-type GaAs can be observed in the spectral region between $\omega_{TO} \sim 268 \text{ cm}^{-1}$ and the coupled LO-phonon-plasmon resonance $\omega_{LPP^+} \sim 300 \text{ cm}^{-1}$. The sharp resonance at $\omega = 297 \text{ cm}^{-1}$ can be attributed to plasmon-phonon-mode induced surface-bound electromagnetic wave propagation at the substrate/buffer interface, as discussed in Ref. 13.

The AlInP₂ layer causes distinct structures in the fir-SE Ψ spectra at 310 cm⁻¹ $\leq \omega \leq 480$ cm⁻¹. As expected from studies of disordered AlInP₂ samples, TO and LO resonances

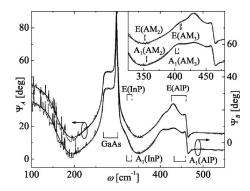


FIG. 1. Experimental (dashed line) and calculated (solid line) fir-SE Ψ spectra for sample E at Φ_a =70°. Ψ_A and Ψ_B denote the fir-SE Ψ spectra taken with the sample $[\bar{1}10]$ axis parallel and perpendicular to the plane of incidence, respectively. The Ψ_A spectrum is shifted by 9° for convenience. The AlInP₂ epilayer InP- and AlP-like TO (solid vertical lines) and LO (dashed vertical lines) modes are indicated by brackets. The inset enlarges the spectral region of AM₂-AM₃.

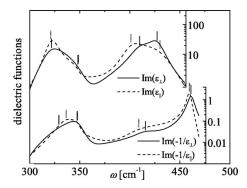


FIG. 2. AlInP₂ MDF's ϵ_{\parallel} and ϵ_{\perp} obtained from the data analysis for sample E. Maxima of $\operatorname{Im}(\epsilon_{\perp})$ and $\operatorname{Im}(\epsilon_{\parallel})$ coincide with the spectral position of the $E(\operatorname{TO})$ and $A_1(\operatorname{TO})$ modes. The corresponding $E(\operatorname{LO})$ and $A_1(\operatorname{LO})$ modes can be observed as maxima of $\operatorname{Im}(-1/\epsilon_{\perp})$ and $\operatorname{Im}(-1\epsilon_{\parallel})$, respectively. $E(\operatorname{TO},\operatorname{LO})$ and $A_1(\operatorname{TO},\operatorname{LO})$ modes are indicated with vertical solid and doted lines, respectively.

of the InP- and AlP-like lattice and two additional modes $(AM_2 \text{ and } AM_3)$ which do not descend from the binary lattice constituents in AlInP₂ can be identified. ¹² In contrast to disordered AlInP₂, differences can be observed between the two sample orientations, reflecting the anisotropic character of the ordered AlInP₂ layer. The difference between $\Psi_{\mathcal{A}}$ and $\Psi_{\mathcal{B}}$ is most notably in the region of 400 cm⁻¹ $\leq \omega \leq$ 460 cm⁻¹ were the AlP(TO,LO) and AM₃(TO,LO) modes occur.

Figure 2 shows the calculated dielectric functions ϵ_{\perp} and ϵ_{\parallel} . The vertical lines indicate the best-fit TO and LO phonon mode frequencies. The differences between the dielectric functions parallel and perpendicular to the ordering direction can be clearly observed at $\omega \sim 330$, 410, and 430 cm⁻¹, reflecting the birefringence of spontaneously ordered AlInP₂ in the vicinity of the InP- and AlP-like lattice and the AM modes. We observe that for partially ordered AlInP₂ the InP- and AlP-like lattice and the AM modes split in A_1 - and E-type modes. For the InP-like and the AM₃ mode, the oscillator strength of the A_1 -type is larger than the E-type vibration. The relation is vice versa for the AlP mode. The A_1 - and E-type mode frequencies of the AM₃ mode differ significantly and deviate from the isotropic AM₃ mode observed in highly disordered AlInP₂ (see Table II and III of Ref. 10).

Figure 3 summarizes the evolution of the E(TO,LO) and $A_1(TO,LO)$ phonon-mode frequencies as a function of η for

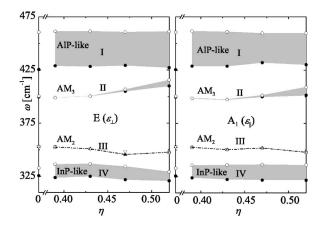


FIG. 3. *E*-(left panel) and A_1 -type (right panel) AlInP₂ phonon modes vs η (solid symbols: TO; open symbols: LO). Four bands attributed to AlP-like, InP-like, and AM_{3,2} phonon modes can be distinguished.

all investigated samples. Four phonon bands can be recognized. Most striking are the changes in the AM₃ band with increasing η where a drastic increase in polarity and anisotropy is observed. In a previous work on disordered $(Al_xGa_{1-x})_{0.52}In_{0.48}P$, we identified AM₂ as likely ordering induced, but the origin of AM₃ remained unclear. 12 It is evident now from Fig. 3 that AM3 is caused by long range atomic ordering, but might also be observed in highly disordered samples due to residual ordering. In highly disordered samples, however, anisotropy and polarity of this mode are very small. The evolution of the other phonon bands is more subtle. The frequencies of the AlP- and InP-like TO and LO phonon modes obtained for the disordered sample agree well with those in the literature. 1,14 Slight changes can be observed in polarity and anisotropy as the degree of ordering increases. This corresponds to the observations of Huang et al., who reported on a variation of Raman scattering intensities of the AlP-like phonon mode in ordered AlInP₂. The ratios of intensities from different modes scaled linearly with the degree of ordering. However, the ordering-induced modes AM2 and AM3 and their splittings have not been reported so far.

In conclusion, we observe a large ordering-induced birefringence in the spectral range of the reststrahlenband of CuPt-type ordered AlInP $_2$ and we report the dielectric functions parallel and perpendicular to the ordering direction. It was obtained that all detectable fir-active phonon modes split upon CuPt-type ordering in modes with A_1 - and E-type symmetries. The previously found AM $_3$ mode shows the most significant ordering dependency. We propose fir-SE as alternative, sensitive, and nondestructive tool for measuring the degree of ordering in AlInP $_2$, as previously demonstrated for $Ga_{0.52}In_{0.48}P$. This is of particular interest because of the indirect-gap behavior of AlInP $_2$, where luminescence experiments do not readily provide the direct band gap properties.

We acknowledge support from the Deutsche Forschungsgemeinschaft under grant SCHUH 133813-1, the National Science Foundation in MRSEC QSPIN at UNL, startup funds from the CoE at UNL, and the J. A. Woollam Foundation.

¹L. Y. Huang, C. H. Chen, Y. F. Chen, W. C. Yeh, and Y. S. Huang, Phys. Rev. B **66**, 073203 (2002).

²A. Zunger, MRS Bull. **22**, 20 (1997).

³J. Humlíček, Thin Solid Films **313–314**, 687 (1998).

⁴T. E. Tiwald, J. A. Woollam, S. Zollner, J. Christiansen, R. B. Gregory, T. Wetteroth, S. Wilson, and A. Powell, Phys. Rev. B **60**, 11464 (1999).

⁵A. Kasic, M. Schubert, S. Einfeldt, D. Hommel, and T. E. Tiwald, Phys. Rev. B 62, 7365 (2000).

⁶M. Schubert, T. Hofmann, and C. M. Herzinger, J. Opt. Soc. Am. A **20**, 347 (2003).

⁷M. Schubert, B. Rheinländer, E. Franke, I. Pietzonka, J. Škriniarová, and V. Gottschalch, Phys. Rev. B **54**, 17616 (1996).

⁸S.-H. Wei and A. Zunger, Phys. Rev. B **57**, 8983 (1998).

⁹M. Schubert, *Infrared Ellipsometry on Semiconductor Layer Structures: Phonons, Plasmons and Polaritons*, Springer Tracts in Modern Physics Vol. 209 (Springer, Berlin, 2004), p. 8.

¹⁰T. Hofmann, V. Gottschalch, and M. Schubert, Phys. Rev. B **66**, 195204 1 (2002)

¹¹G. E. Jellison, Thin Solid Films **313–314**, 33 (1998).

¹²T. Hofmann, G. Leibiger, V. Gottschalch, I. Pietzonka, and M. Schubert, Phys. Rev. B **64**, 155206 (2001).

¹³M. Schubert, T. Hofmann, and J. Šik, Phys. Rev. B **71**, 35324 (2005).

¹⁴H. Asahi, S. Emura, and S. Gonda, J. Appl. Phys. 65, 5007 (1989).